JJMS **18**, No. 4, 635-647 (2025)

Jordan Journal of Mathematics and Statistics.
Yarmouk University

DOI:https://doi.org/10.47013/18.4.11

Kumaraswamy Sine Inverted Rayleigh distribution : Properties and Application to Bladder Cancer Data

Abdulhameed Ado Osi[1,*], *Usman Abubakar*[2], *and Muftahu Zubairu Ringim*[3]

[1] Department of Statistics, Aliko Dangote University of Science and Technology, Wudil, Nigeria
[2] Department of Statistics, Jigawa State Polytechnic, Dutse, Nigeria
[3] Department of Mathematics, Aliko Dangote University of Science and Technology, Wudil, Nigeria

Received: June 25, 2024 Accepted : May 8, 2025

Abstract: In this work, we introduce the Kumaraswamy Sine Inverted Rayleigh (KWSIR) distribution as an extension of the classical Inverse Rayleigh distribution, offering greater flexibility in modeling real-world data. The KWSIR distribution combines the Kumaraswamy and Sine Inverted Rayleigh distributions, resulting in a unimodal, right-skewed probability density function and an increasing or J-shaped hazard rate function. We explore key statistical properties, including the probability density function, cumulative distribution function, quantile function, moments, incomplete moments, entropy measures, and order statistics. Parameter estimation is conducted using the maximum likelihood method. To illustrate its applicability, we analyze a real-world dataset on bladder cancer, demonstrating the superior fitting performance of the KWSIR distribution.

Keywords: Probability distribution; maximum likelihood estimation; moments, moment generating function.

2010 Mathematics Subject Classification. 26A25; 26A35.

1 Introduction

Traditional probability distributions often fail to accurately capture the full range of variability observed in hazard rates and survival functions across various domains, including reliability engineering, survival analysis, and lifetime data modeling [4]. This limitation has led to a growing interest in developing more flexible and generalized distributions that can better accommodate diverse data structures. One of the most effective approaches involves introducing additional shape parameters into baseline models, allowing for greater adaptability in fitting complex datasets. Several generalized families of probability distributions have been proposed in the literature to address these challenges. For example, the exponentiated-G family gained popularity after [10] extended the exponentiated exponential distribution. The beta-G family was introduced by [8], while the gamma-G family was developed by [16]. Additionally, the Marshall-Olkin-G family, proposed by [11] and Kumaraswamy G family by [7], have been widely applied in various statistical analyses.

Despite the advancements in generalized probability distributions, there is still a need for flexible models that can accurately describe real-world data, particularly in cases where traditional distributions fall short. The incorporation of trigonometric functions into probability distributions has emerged as an effective strategy for enhancing their flexibility. The recently introduced G-class of trigonometric distributions has demonstrated significant potential in improving data modeling by integrating sine and cosine transformations with existing generators [4]. Several researchers have explored the application of trigonometric-based generalizations in statistical modeling. For instance, [9] introduced the sine extended odd Fréchet-G family, which showed promise in handling complete and censored data. Similarly, [6] developed the sine Kumaraswamy-G family, while [1] investigated the sine Topp-Leone-G family. The alpha-sine-G family, proposed by [4], extended the sine transformation by adding an extra parameter, further enhancing its adaptability. Other notable contributions include the Sin-G class of distributions explored by [15], the weighted cosine-G family introduced by [14], the cosine-sine transformation-based distributions developed by [5] and Transmuted Cosine Topp-Leone G-Family by [13].

* Corresponding author e-mail: aaosi@kustwudil.edu.ng

© 2025 YU
Deanship of Research and Graduate Studies, Yarmouk University, Irbid, Jordan.

Building upon these advancements, this study aims to introduce a novel extension of the Inverted Rayleigh distribution by incorporating the sine-G and Kumaraswamy-G families. Specifically, we propose the Kumaraswamy Sine Inverted Rayleigh (KWSIR) distribution, which is expected to provide improved flexibility and modeling capability, particularly for lifetime data analysis. This research will investigate the fundamental statistical properties of the KWSIR distribution, including its moments, entropy, hazard function, and survival function. Additionally, we will evaluate its performance using real-world data to demonstrate its practical applicability and superiority over existing models.

1.1 Kumaraswamy-G Family, Sine-G Family and inverted Rayleigh distribution

The CDF of Kumaraswamy-G is given as;

$$F(x) = 1 - \{1 - G(x)^{a}\}^{b}; \quad x \in \mathbb{R}. \tag{1}$$

The CDF of Sine-G family of Distribution is given as;

$$F(x) = Sin\left\{\frac{\pi}{2}G(x)\right\} \quad x \in \mathbb{R}. \tag{2}$$

And the CDF of Inverted Rayleigh is given by;

$$F(x) = e^{\frac{-\lambda}{x^2}} \quad x > 0. \tag{3}$$

2 Kumaraswamy Sine Inverted Rayleigh (KWSIR) distribution

The cumulative distribution function and Probability density function fo Kumaraswamy Sine Inverted Rayleigh (KWSIR) distribution can be obtained by combining Eq.(1), Eq.(2) and Eq.(3) which gives,

$$F(x) = 1 - \left\{1 - \left\{Sin\frac{\pi}{2}e^{\frac{-\lambda}{x^2}}\right\}^{\alpha}\right\}^{\theta}; \quad x \in \mathbb{R}. \tag{4}$$

The corresponding PDF of Kumaraswamy Sine Inverted Rayliegh distribution is

$$f(x) = \pi\alpha\lambda\theta x^{-3}e^{\frac{-\lambda}{x^2}}\left\{Cos\frac{\pi}{2}e^{\frac{-\lambda}{x^2}}\right\}\left\{Sin\frac{\pi}{2}e^{\frac{-\lambda}{x^2}}\right\}^{\alpha-1}\left\{1 - \left\{Sin\frac{\pi}{2}e^{\frac{-\lambda}{x^2}}\right\}^{\alpha}\right\}^{\theta-1}; \quad x \in \mathbb{R}. \tag{5}$$

© 2025 YU
Deanship of Research and Graduate Studies, Yarmouk University, Irbid, Jordan.

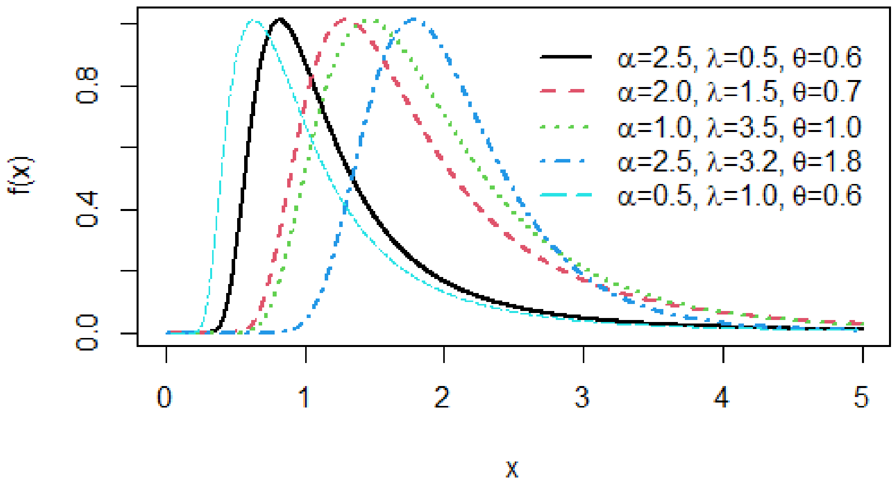

Fig. 1: The PDF plot of KWSIR

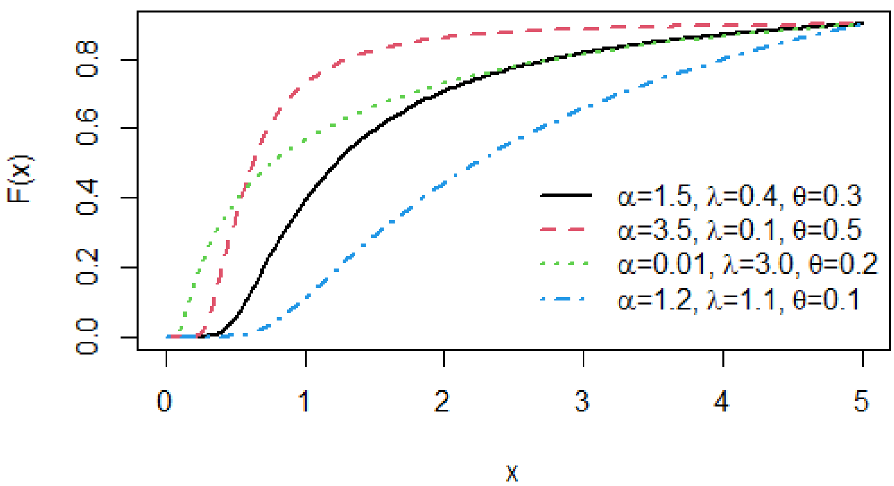

Fig. 2: The CDF plot of KWSIR

3 Statistical Properties of KWSIR

This section examines and identifies the fundamental properties of the Kumaraswamy Sine Inverted Rayleigh (KWSIR) distribution, which play a crucial role in understanding its behavior and applicability in real-world scenarios. By analyzing

© 2025 YU
Deanship of Research and Graduate Studies, Yarmouk University, Irbid, Jordan.

these properties, we gain deeper insights into the distribution's flexibility, suitability for various datasets, and potential for modeling diverse real-life phenomena. The key properties explored in this section include:

3.1 Survival function and hazard rate function of KWSIR

In this part, we derive the survival function and hazard rate function of KWSIR distribution.

$$S(x) = \left\{1 - \left\{Sin\frac{\pi}{2}e^{\frac{-\lambda}{x^2}}\right\}^{\alpha}\right\}^{\theta}, \tag{6}$$

$$H(x) = \frac{\pi\alpha\lambda\theta x^{-3}e^{\frac{-\lambda}{x^2}}\left\{Cos\frac{\pi}{2}e^{\frac{-\lambda}{x^2}}\right\}\left\{Sin\frac{\pi}{2}e^{\frac{-\lambda}{x^2}}\right\}^{\alpha-1}}{\left\{1 - \left\{Sin\frac{\pi}{2}e^{\frac{-\lambda}{x^2}}\right\}^{\alpha}\right\}}. \tag{7}$$

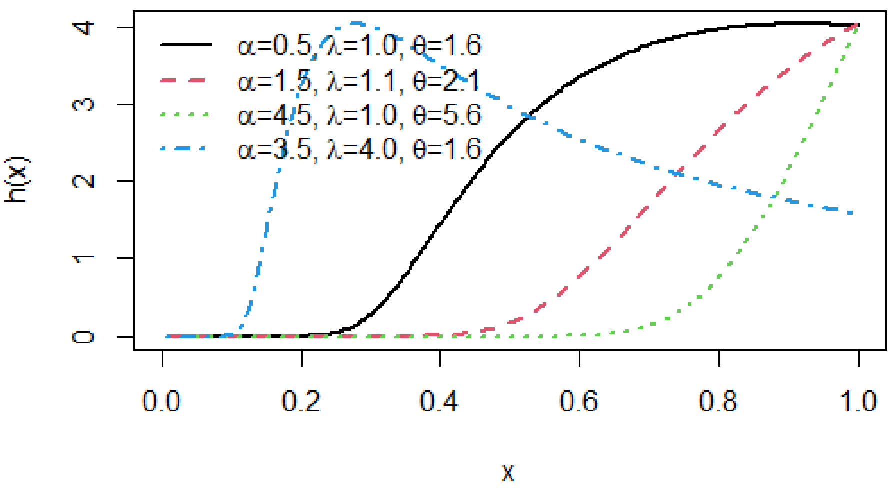

Fig. 3: The hazard function plot for KWSIR

© 2025 YU
Deanship of Research and Graduate Studies, Yarmouk University, Irbid, Jordan.

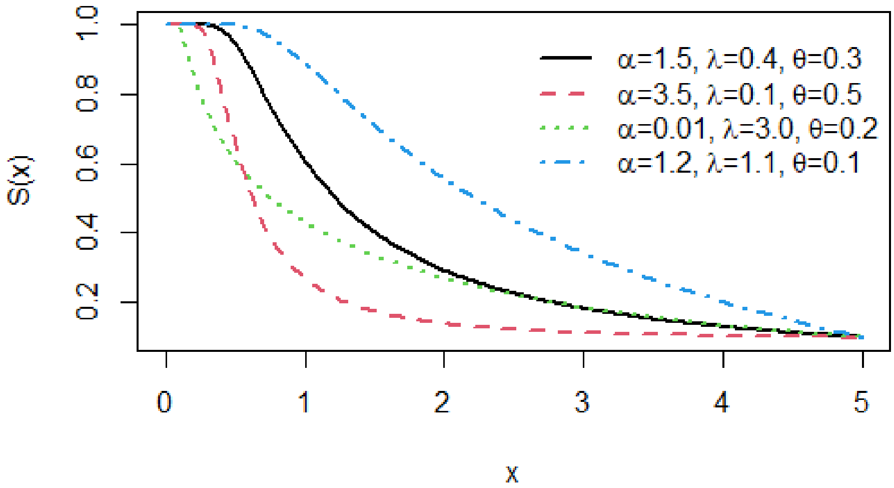

Fig. 4: The Survival function plot for KWSIR

Fig.1, Fig.2, Fig.3 and Fig.4 show plots of the PDF, CDF, hazard rate and survival functions for the KWSIR distribution. Fig.1 displays unimodal curves that are right-skewed. Therefore, the hazard rate shape of the KWSIR distribution could be increasing and reversed bathtub, depending on the parameter values, as illustrated in Fig.3.

3.2 Quantile function of KWSIR

Random samples from the KWSIR distribution can be generated using the quantile function (QF), which is the inverse of the cumulative distribution function (CDF). Mathematically, the quantile function is expressed as

$$Q(u) = F^{-1}(u). \tag{8}$$

Thus, the QF of the KWSIR distribution can be derived as follows:

$$Qu = \left\{ \frac{-\lambda}{log\left\{ \frac{2}{\pi} Arcsine\left(1-(1-u)^{\frac{1}{\theta}}\right)^{\frac{1}{\alpha}} \right\}} \right\}^{\frac{1}{2}}. \tag{9}$$

However, other important properties of the KWSIR distribution include entropy, moments, moment generating function, and order statistics, which are derived below.

3.3 Moments and Moment Generating Function of KWSIR

This section presents the moments and the Moment Generating Function (MGF) of the KWSIR distribution. Moments are essential for understanding the key characteristics of a distribution, such as central tendency, dispersion, skewness, and kurtosis.

Let X be a random variable with probability density function (PDF) $f(x)$. The rth moment of X is given by:

$$\mu_r = E(X^r) = \int_{-\infty}^{\infty} x^r f(x) dx. \tag{10}$$

© 2025 YU
Deanship of Research and Graduate Studies, Yarmouk University, Irbid, Jordan.

Substituting the PDF of the KWSIR distribution into the above equation, we obtain:

$$\mu_r = \pi\alpha\lambda\theta \int_0^\infty x^{r-3} e^{\frac{-\lambda}{x^2}} \left\{\cos\left(\frac{\pi}{2}e^{\frac{-\lambda}{x^2}}\right)\right\} \left\{\sin\left(\frac{\pi}{2}e^{\frac{-\lambda}{x^2}}\right)\right\}^{\alpha-1} \left\{1-\left(\sin\frac{\pi}{2}e^{\frac{-\lambda}{x^2}}\right)^{\alpha}\right\}^{\theta-1} dx. \tag{11}$$

Expanding using a power series representation:

$$\mu_r = \sum_{i=0}^{\infty} \int_0^\infty \frac{\pi\alpha\lambda^{1+i}\theta(-1)^i}{i!} x^{r-3-2i} \left\{\cos\left(\frac{\pi}{2}e^{\frac{-\lambda}{x^2}}\right)\right\} \left\{\sin\left(\frac{\pi}{2}e^{\frac{-\lambda}{x^2}}\right)\right\}^{\alpha-1} \left\{1-\left(\sin\frac{\pi}{2}e^{\frac{-\lambda}{x^2}}\right)^{\alpha}\right\}^{\theta-1} dx. \tag{12}$$

Since:

$$e^{\frac{-\lambda}{x^2}} = \sum_{i=0}^{\infty} \frac{(-1)^i\lambda^i}{x^{2i} i!}, \tag{13}$$

it follows that:

$$\mu_r = \sum_{i=0}^{\infty} \gamma\omega. \tag{14}$$

where:

$$\gamma = \int_0^\infty x^{r-3-2i} \left\{\cos\left(\frac{\pi}{2}e^{\frac{-\lambda}{x^2}}\right)\right\} \left\{\sin\left(\frac{\pi}{2}e^{\frac{-\lambda}{x^2}}\right)\right\}^{\alpha-1} \left\{1-\left(\sin\frac{\pi}{2}e^{\frac{-\lambda}{x^2}}\right)^{\alpha}\right\}^{\theta-1} dx, \tag{15}$$

and

$$\omega = \frac{\pi\alpha\lambda^{1+i}\theta(-1)^i}{i!}. \tag{16}$$

Moment Generating Function of KWSIR

The moment generating function (MGF) of the KWSIR distribution is given by:

$$M_X(t) = E(e^{tX}) = \int_{-\infty}^{\infty} e^{tX} f(x)dx. \tag{17}$$

Substituting the PDF of KWSIR, we obtain:

$$M_X(t) = \int_0^\infty \pi\alpha\lambda\theta x^{-3} e^{tX} e^{\frac{-\lambda}{x^2}} \left\{\cos\left(\frac{\pi}{2}e^{\frac{-\lambda}{x^2}}\right)\right\} \left\{\sin\left(\frac{\pi}{2}e^{\frac{-\lambda}{x^2}}\right)\right\}^{\alpha-1} \left\{1-\left(\sin\frac{\pi}{2}e^{\frac{-\lambda}{x^2}}\right)^{\alpha}\right\}^{\theta-1} dx. \tag{18}$$

Using power series expansions:

$$e^{tX} = \sum_{i=0}^{\infty} \frac{t^i X^i}{i!}, \quad e^{\frac{-\lambda}{x^2}} = \sum_{j=0}^{\infty} \frac{(-1)^j\lambda^j}{x^{2j} j!}. \tag{19}$$

Thus,

$$e^{tX} e^{\frac{-\lambda}{x^2}} = \sum_{i=0}^{\infty}\sum_{j=0}^{\infty} \frac{(-1)^j\lambda^j t^i X^{i-2j}}{x^{2j} i! j!}. \tag{20}$$

Substituting equation (18) into (20), we obtain:

$$M_X(t) = \sum_{i=0}^{\infty}\sum_{j=0}^{\infty} \int_0^\infty \frac{\pi\theta(-1)^j\lambda^{j+1}t^i x^{i-2j-3}}{x^{2j} i! j!} \left\{\cos\left(\frac{\pi}{2}e^{\frac{-\lambda}{x^2}}\right)\right\} \left\{\sin\left(\frac{\pi}{2}e^{\frac{-\lambda}{x^2}}\right)\right\}^{\alpha-1} \left\{1-\left(\sin\frac{\pi}{2}e^{\frac{-\lambda}{x^2}}\right)^{\alpha}\right\}^{\theta-1} dx. \tag{21}$$

Thus, we can express the MGF as:

$$M_X(t) = \sum_{i=0}^{\infty}\sum_{j=0}^{\infty} \psi\rho. \tag{22}$$

© 2025 YU
Deanship of Research and Graduate Studies, Yarmouk University, Irbid, Jordan.

where:

$$\psi = \int_0^\infty x^{i-2j-3} \left\{ \cos\left(\frac{\pi}{2} e^{\frac{-\lambda}{x^2}}\right) \right\} \left\{ \sin\left(\frac{\pi}{2} e^{\frac{-\lambda}{x^2}}\right) \right\}^{\alpha-1} \left\{ 1 - \left(\sin\frac{\pi}{2} e^{\frac{-\lambda}{x^2}}\right)^{\alpha} \right\}^{\theta-1} dx. \tag{23}$$

and

$$\rho = \frac{\pi\theta(-1)^j \lambda^{j+1} t^i}{x^{2j} i! j!}. \tag{24}$$

3.4 Renyi's Entropy of KWSIR

Entropy is a fundamental concept in statistical analysis that enables the calculation of uncertainty associated with different outcomes. It has numerous applications in mathematical analysis. In this study, we focus on Renyi entropy as our chosen entropy metric.

Let X be a random variable with a probability density function (PDF) $f(x)$. The Renyi entropy is given by:

$$RE = I_X = \frac{1}{1-\delta} \log \int_{-\infty}^{\infty} f(x)^\delta dx. \tag{25}$$

Substituting the PDF of the KWSIR distribution:

$$RE = \frac{1}{1-\delta} \log \int_0^\infty (ab)^\delta dx. \tag{26}$$

Expanding,

$$RE = \frac{1}{1-\delta} \left[\delta \log a + \log \int_0^\infty b^\delta dx \right]. \tag{27}$$

where:

$$a = \pi\theta\lambda\alpha,$$

$$b = x^{-3} e^{-\frac{\lambda}{x^2}} \cos\left(\frac{\pi}{2} e^{-\frac{\lambda}{x^2}}\right) \sin^{\alpha-1}\left(\frac{\pi}{2} e^{-\frac{\lambda}{x^2}}\right) \left(1 - \sin^{\alpha}\left(\frac{\pi}{2} e^{-\frac{\lambda}{x^2}}\right)\right)^{\theta-1}.$$

3.5 Order Statistics of KWSIR

Consider a random sample $x_1, x_2, \ldots, x_n$ from the KWSIR distribution, with order statistics $x_{1:n} \leq x_{2:n} \leq \cdots \leq x_{n:n}$. The probability density function (PDF) of the ith order statistic is given by:

$$f_{(i,n)}(x) = \frac{n!}{(i-1)!(n-i)!} f(x)[F(x)]^{i-1}[1-F(x)]^{n-i}. \tag{28}$$

Using the power series expansion:

$$[1-F(x)]^{n-i} = \sum_{j=0}^{n-i} (-1)^j \binom{n-i}{j} [F(x)]^j. \tag{29}$$

Substituting this into the equation:

$$f_{(i,n)}(x) = \frac{n!}{(i-1)!(n-i)!} \sum_{j=0}^{n-i} \binom{n-i}{j} (-1)^j f(x)[F(x)]^{i+j-1}. \tag{30}$$

Rewriting:

$$f_{(i,n)}(x) = \sum_{j=0}^{n-i} \binom{n-i}{j} \frac{n!\kappa\pi\alpha\lambda\theta(-1)^j}{(i-1)!(n-i-j)!}. \tag{31}$$

© 2025 YU
Deanship of Research and Graduate Studies, Yarmouk University, Irbid, Jordan.

where:

$$\kappa = x^{-3} e^{-\frac{\lambda}{x^2}} \cos\left(\frac{\pi}{2} e^{-\frac{\lambda}{x^2}}\right) \sin^{\alpha-1}\left(\frac{\pi}{2} e^{-\frac{\lambda}{x^2}}\right) \left(1-\sin^{\alpha}\left(\frac{\pi}{2} e^{-\frac{\lambda}{x^2}}\right)\right)^{\theta-1} \left[1-\left(1-\sin^{\alpha}\left(\frac{\pi}{2} e^{-\frac{\lambda}{x^2}}\right)\right)^{\theta}\right]^{i+j-1}.$$

4 Maximum Likelihood Estimation

In this section, we consider the maximum likelihood estimators (MLE) for the KWSIR distribution. Let $x_1, x_2, \ldots, x_n$ be a random sample from the KWSIR family of distributions with the probability density function (PDF) given in equation (5), where the parameter vector is defined as:

$$\eta = (\alpha, \lambda, \theta)^T.$$

The log-likelihood function for the KWSIR distribution, based on a sample of size n, is given by:

$$\begin{aligned} l(\eta) = {} & n\log\pi + n\log\alpha + n\log\lambda + n\log\theta + \sum_{i=1}^{n} x_i^{-3} + \sum_{i=1}^{n}\left(\frac{-\lambda}{x_i^2}\right) \\ & + \sum_{i=1}^{n}\log\left\{\cos\left(\frac{\pi}{2} e^{\frac{-\lambda}{x_i^2}}\right)\right\} \\ & + (\alpha-1)\sum_{i=1}^{n}\log\left\{\sin\left(\frac{\pi}{2} e^{\frac{-\lambda}{x_i^2}}\right)\right\} \\ & + (\theta-1)\sum_{i=1}^{n}\log\left\{1-\left(\sin\left(\frac{\pi}{2} e^{\frac{-\lambda}{x_i^2}}\right)\right)^{\alpha}\right\}. \end{aligned} \tag{32}$$

The first-order derivatives (score functions) for the MLEs are:
Derivative with respect to α

$$\begin{aligned} \frac{dl}{d\alpha} = {} & \frac{n}{\alpha} + \sum_{i=1}^{n}\log\left\{\sin\left(\frac{\pi}{2} e^{\frac{-\lambda}{x_i^2}}\right)\right\} \\ & + (\theta-1)\sum_{i=1}^{n}\frac{\pi\alpha\lambda e^{\frac{-\lambda}{x_i^2}}\cos\left(\frac{\pi}{2} e^{\frac{-\lambda}{x_i^2}}\right)\left(\sin\left(\frac{\pi}{2} e^{\frac{-\lambda}{x_i^2}}\right)\right)^{\alpha-1}}{x_i^2\left(1-\left(\sin\left(\frac{\pi}{2} e^{\frac{-\lambda}{x_i^2}}\right)\right)^{\alpha}\right)}. \end{aligned} \tag{33}$$

Derivative with respect to θ

$$\frac{dl}{d\theta} = \frac{n}{\theta} + \sum_{i=1}^{n}\log\left\{1-\left(\sin\left(\frac{\pi}{2} e^{\frac{-\lambda}{x_i^2}}\right)\right)^{\alpha}\right\}. \tag{34}$$

Derivative with respect to λ

© 2025 YU

$$\frac{dl}{d\lambda} = \frac{n}{\lambda} + \sum_{i=1}^{n}\left(\frac{1}{x_i^2}\right) + \sum_{i=1}^{n}\frac{\pi e^{\frac{-\lambda}{x_i^2}}\sin\left(\frac{\pi}{2}e^{\frac{-\lambda}{x_i^2}}\right)}{2x_i^2\cos\left(\frac{\pi}{2}e^{\frac{-\lambda}{x_i^2}}\right)} - (\alpha-1)\sum_{i=1}^{n}\frac{\pi e^{\frac{-\lambda}{x_i^2}}\cos\left(\frac{\pi}{2}e^{\frac{-\lambda}{x_i^2}}\right)}{2x_i^2\sin\left(\frac{\pi}{2}e^{\frac{-\lambda}{x_i^2}}\right)} + (\theta-1)\sum_{i=1}^{n}\frac{\alpha e^{\frac{-\lambda}{x_i^2}}\left(\sin\left(\frac{\pi}{2}e^{\frac{-\lambda}{x_i^2}}\right)\right)^{\alpha-1}\cos\left(\frac{\pi}{2}e^{\frac{-\lambda}{x_i^2}}\right)}{x_i^2\left(1-\left(\sin\left(\frac{\pi}{2}e^{\frac{-\lambda}{x_i^2}}\right)\right)^{\alpha}\right)}. \tag{35}$$

The MLEs for α, λ, and θ are obtained by solving these nonlinear equations iteratively. Common methods to solve such equations include: The Newton-Raphson method, which iteratively updates parameter estimates using:

$$\eta^{(t+1)} = \eta^{(t)} - \left[H(\eta^{(t)})\right]^{-1} S(\eta^{(t)}),$$

where $S(\eta)$ is the score function (vector of first derivatives) and $H(\eta)$ is the Hessian matrix (matrix of second derivatives).

5 Simulation Study

In this section, we conduct a simulation study to evaluate the performance of the maximum likelihood estimation (MLE) method for the KWSIR distribution. We consider three key performance metrics: the mean of the estimates, bias, and Mean Squared Error (MSE). These metrics provide insights into the accuracy and consistency of the MLE under different parameter settings.

Mean of the Estimates

The mean of the estimated parameters over S replications is calculated as follows:

$$\bar{\lambda} = \frac{1}{S}\sum_{j=1}^{S}\hat{\lambda}_j, \quad \bar{\alpha} = \frac{1}{S}\sum_{j=1}^{S}\hat{\alpha}_j, \quad \bar{\theta} = \frac{1}{S}\sum_{j=1}^{S}\hat{\theta}_j. \tag{36}$$

Bias

The bias measures the deviation of the average estimated parameter from its true value:

$$\text{Bias}(\bar{\lambda}) = \bar{\lambda} - \lambda, \quad \text{Bias}(\bar{\alpha}) = \bar{\alpha} - \alpha, \quad \text{Bias}(\bar{\theta}) = \bar{\theta} - \theta. \tag{37}$$

Mean Squared Error (MSE)

The MSE quantifies the accuracy of the estimates by computing the average squared differences between the estimated and true values:

$$MSE(\bar{\lambda}) = \frac{1}{S}\sum_{j=1}^{S}\left(\hat{\lambda}_j - \lambda\right)^2, \tag{38}$$

$$MSE(\bar{\alpha}) = \frac{1}{S}\sum_{j=1}^{S}\left(\hat{\alpha}_j - \alpha\right)^2, \tag{39}$$

© 2025 YU
Deanship of Research and Graduate Studies, Yarmouk University, Irbid, Jordan.

$$MSE(\bar{\theta}) = \frac{1}{S}\sum_{j=1}^{S}\left(\hat{\theta}_j - \theta\right)^2. \tag{40}$$

We evaluate the MLE performance under two different parameter settings:

–**First trial:** $\lambda = 1.8$, $\alpha = 1.5$, $\theta = 1.2$.
–**Second trial:** $\lambda = 1.4$, $\alpha = 2.0$, $\theta = 2.7$.

Random samples were generated using the quantile function of the KWSIR distribution. For each trial, we generated samples of size $n = 20, 50, 100, 250, 500, 1000$, with 1000 replications. The means, biases, and mean squared errors (MSEs) of the estimates were computed. The results are summarized in Table 1.

Based on the Monte Carlo simulation results, we conclude that our model consistently produces accurate parameter estimates, as the bias and RMSE values decrease with increasing sample size.

Table 1: Simulation results for different parameter values

		Trial 1: $\lambda = 1.8, \alpha = 1.5, \theta = 1.2$			Trial 2: $\lambda = 1.4, \alpha = 2.0, \theta = 2.7$		
Sample Size	Metric	λ	α	θ	λ	α	θ
$n = 20$	Mean	1.7878	1.6938	1.5358	1.9591	2.5305	3.4886
	Bias	-0.0122	0.1938	0.3358	0.5591	0.5305	0.7886
	MSE	0.7450	0.8828	0.7988	0.8733	1.1335	2.1961
$n = 50$	Mean	1.6821	1.5868	1.3316	1.8805	2.3835	2.8984
	Bias	-0.1179	0.0868	0.1316	0.4805	0.3835	0.1984
	MSE	0.6092	0.6534	0.3661	0.6637	0.7952	0.8848
$n = 100$	Mean	1.6030	1.5799	1.2699	1.8340	2.3338	2.7442
	Bias	-0.1970	0.0799	0.0629	0.4534	0.3338	0.0442
	MSE	0.5294	0.5363	0.3661	0.5832	0.6345	0.5543
$n = 250$	Mean	1.5938	1.5116	1.2311	1.8841	2.2288	2.6793
	Bias	-0.2062	0.0116	0.0311	0.4841	0.2288	-0.0207
	MSE	0.4348	0.4099	0.1494	0.5719	0.4693	0.3556
$n = 500$	Mean	1.5769	1.4860	1.2206	1.8717	2.2090	2.6448
	Bias	-0.2231	-0.0140	0.0206	0.4717	0.2090	-0.0552
	MSE	0.3799	0.3237	0.1056	0.5293	0.3856	0.2522
$n = 1000$	Mean	1.5890	1.4509	1.2221	1.8477	2.1572	2.6518
	Bias	-0.2110	-0.0491	0.0221	0.4477	0.1572	-0.0482
	MSE	0.3411	0.2649	0.0844	0.5194	0.3080	0.1929

6 Application to Bladder Cancer Data

In this study, we analyze real-world data on the remission times (in months) of a randomly selected sample of 128 bladder cancer patients. The dataset, extracted from [2], is given as follows:

0.08, 2.09, 3.48, 4.87, 6.94, 8.66, 13.11, 23.63, 0.20, 2.23, 3.52, 4.98, 6.97, 9.02, 13.29, 0.40, 2.26, 3.57, 5.06, 7.09, 9.22, 13.80, 25.74, 0.50, 2.46, 3.64, 5.09, 7.26, 9.47, 14.24, 25.82, 0.51, 2.54, 3.70, 5.17, 7.28, 9.74, 14.76, 26.31, 0.81, 2.62, 3.82, 5.32, 7.32, 10.06, 14.77, 32.15, 2.64, 3.88, 5.32, 7.39, 10.34, 14.83, 34.26, 0.90, 2.69, 4.18, 5.34, 7.59, 10.66, 15.96, 36.66, 1.05, 2.69, 4.23, 5.41, 7.62, 10.75, 16.62, 43.01, 1.19, 2.75, 4.26, 5.41, 7.63, 17.12, 46.12, 1.26, 2.83, 4.33, 5.49, 7.66, 11.25, 17.14, 79.05, 1.35, 2.87, 5.62, 7.87, 11.64, 17.36, 1.40, 3.02, 4.34, 5.71, 7.93, 1.46, 18.10, 11.79, 4.40, 5.85, 8.26, 11.98, 19.13, 1.76, 3.25, 4.50, 6.25, 8.37, 12.02, 2.02, 13.31, 4.51, 6.54, 8.53, 12.03, 20.28, 2.02, 3.36, 12.07, 6.76, 21.73, 2.07, 3.36, 6.93, 8.65, 12.63, 22.69.

© 2025 YU
Deanship of Research and Graduate Studies, Yarmouk University, Irbid, Jordan.

To evaluate the fit of different statistical models to the bladder cancer dataset, we employed several goodness-of-fit measures and information criteria. These included:

- The log-likelihood function evaluated at the Maximum Likelihood Estimates (MLEs) - Akaike Information Criterion (AIC) - Bayesian Information Criterion (BIC) - Corrected Akaike Information Criterion (CAIC) - Anderson-Darling statistic (A^*) - Cramer-von Mises statistic (W^*) - Kolmogorov-Smirnov (K-S) statistic

Generally, lower values of these criteria indicate a better model fit.

$$AIC = -2L + 2k \tag{41}$$

$$BIC = -2L + k\log(n) \tag{42}$$

$$CAIC = -2L + \frac{2kn}{n-k-1} \tag{43}$$

Where L is log-likelihood, k is the number of parameters and n is the sample size.

Table 2: Information Criteria Measures for the Fitted Models

Distribution	$\hat{\alpha}$	$\hat{\lambda}$	$\hat{\theta}$	$\hat{\gamma}$	$\hat{LL}$	AIC	CAIC	BIC
KWSIR	0.0191	0.1219	4.6339	-	-476.254	960.508	960.833	971.916
SIR	1.000	1.000	1.172	-	-1151.11	2303.3	2308.49	2316.865
KWIR	0.3493	0.1762	0.3496	-	-506.997	1017.993	1018.08	1024.697
MOTLW	0.4961	0.1762	0.4961	0.4961	-506.997	1021.993	1022.319	1033.402

Table 3: Goodness-of-Fit Measures for the Fitted Models

Distribution	K-S	A^*	W^*	P-value
KWSIR	0.2974	6.3912	1.0511	0.6517
SIR	0.8147	12.2999	2.2057	0.1276
KWIR	0.3532	11.9929	2.1269	0.4508
MOTLW	0.3532	11.9933	2.1270	0.5576

This section presents a numerical evaluation of the performance of the Kumaraswamy-Sine Inverse Rayleigh (KWSIR) distribution alongside other competing models: the Sine Inverse Rayleigh (SIR), the Kumaraswamy Inverse Rayleigh (KWIR), and the Marshall-Olkin Topp-Leone Weibull (MOTLW) distributions.

Table 2 summarizes the MLEs of the model parameters, log-likelihood (LL), AIC, CAIC, and BIC values. Table 3 presents the goodness-of-fit statistics, including the Anderson-Darling, Cramer-von Mises, and Kolmogorov-Smirnov tests along with their respective p-values.

The results indicate that the KWSIR model outperforms the other distributions based on information criteria and the Kolmogorov-Smirnov (K-S) statistic. Furthermore, the KWSIR model exhibits the highest p-value for the K-S test, suggesting that it provides the best overall fit for the bladder cancer dataset. Fig. 5 visually illustrates the predicted PDF for the fitted models, further emphasizing the superior performance of the KWSIR model over alternative distributions.

© 2025 YU
Deanship of Research and Graduate Studies, Yarmouk University, Irbid, Jordan.

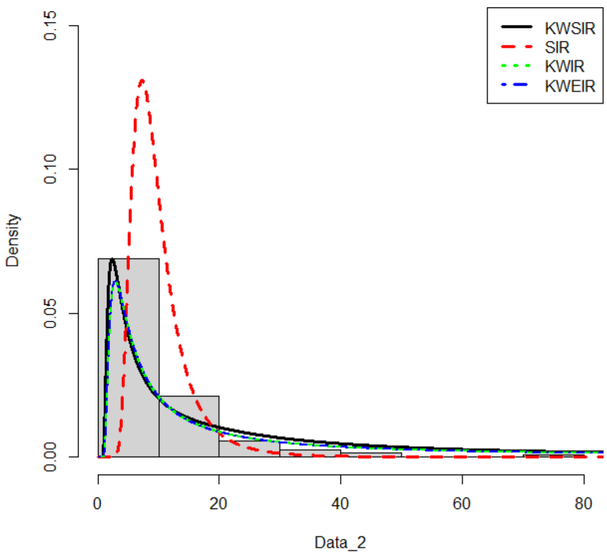

Fig. 5: Fitted Pdf

Conclusion

In this paper, we introduced the Kumaraswamy Inverted Rayleigh (KWSIR) distribution and conducted a comprehensive study of its statistical properties. Specifically, we derived its quantile function, entropy, hazard rate function, survival function, moments, moment-generating function, and order statistics, demonstrating its flexibility and applicability in modeling real-world data. To estimate the parameters of the KWSIR distribution, we employed the maximum likelihood estimation (MLE) method, ensuring robust and efficient parameter estimation. To assess the effectiveness of the proposed distribution, we conducted extensive numerical experiments, including both theoretical analysis and simulation studies. The performance of the KWSIR distribution was compared against other well-established competing models, using goodness-of-fit measures and various information criteria such as the Akaike Information Criterion (AIC), the Corrected Akaike Information Criterion (CAIC), and the Bayesian Information Criterion (BIC). The results of these comparisons consistently indicated that the KWSIR distribution provided a significantly better fit to the bladder cancer remission dataset than the alternative models. Overall, the findings of this study highlight the KWSIR distribution as a promising and effective tool for modeling lifetime and reliability data. Its strong theoretical foundation, combined with its superior empirical performance, suggests its potential applicability in the field of medical research.

Declarations

Competing interests: The authors declare no conflicts of interest related to this study.
Authors' contributions: All authors contributed to the study conception and design.
Funding: The authors did not receive any funding for this research.
Availability of data and materials: The data supporting the findings of this study are included within the manuscript.
Acknowledgments: The authors would like to thank the reviewers for their valuable and insightful suggestions.

References

[1] Al-Babtain, Abdulhakim A and Elbatal, Ibrahim and Chesneau, Christophe and Elgarhy, Mohammed.Sine Topp-Leone-G family of distributions: Theory and applications. *Open Physics*,**18(1)**,(2020), 574–593.

[2] Almetwally, Ehab M and Kilai, Mutua and Aldallal, Ramy. X-Gamma Lomax Distribution with Different Applications. *Journal of Business and Environmental Sciences*,**1(1)**(2022), 129–140.

© 2025 YU
Deanship of Research and Graduate Studies, Yarmouk University, Irbid, Jordan.

[3] Alzaatreh, Ayman and Kazempoor, Jaber and Nadi, Adel Ahmadi.Weighted multimodal family of distributions with sine and cosine weight functions. *Heliyon***6(8)**(2020).

[4] Benchiha, SidAhmed and Sapkota, Laxmi Prasad and Al Mutairi, Aned and Kumar, Vijay and Khashab, Rana H and Gemeay, Ahmed M and Elgarhy, Mohammed and Nassr, Said G. A new sine family of generalized distributions: Statistical inference with applications. *Mathematical and Computational Applications*,**28(4)**(2023), 83.

[5] Chesneau, Christophe and Bakouch, Hassan S and Hussain, Tassaddaq. A new class of probability distributions via cosine and sine functions with applications. *Communications in Statistics-Simulation and Computation*,**48(8)**(2019), 2287–2300.

[6] Chesneau, Christophe and Jamal, Farrukh. The sine Kumaraswamy-G family of distributions. *Journal of Mathematical Extension*,**28**(2020).

[7] Cordeiro, Gauss M and de Castro, Mário.A new family of generalized distributions. *Journal of statistical computation and simulation*,**81(7)**(2011).

[8] Eugene, Nicholas and Lee, Carl and Famoye, Felix. Beta-normal distribution and its applications. *Communications in Statistics-Theory and methods*,**31(4)**(2002), 497–512.

[9] Jamal, Farrukh and Chesneau, Christophe and Aidi, Khaoula. The sine extended odd Fréchet-G family of distribution with applications to complete and censored data. *Mathematica slovaca*,**7(4)**(2021), 961–982.

[10] Kundu, Debasis and Gupta, Rameshwar D. An extension of the generalized exponential distribution. *Statistical Methodology*,**8(6)**(2011), 485–496.

[11] Marshall, Albert W and Olkin, Ingram. A new method for adding a parameter to a family of distributions with application to the exponential and Weibull families. *Biometrika*,**84(3)**(1997), 641–652.

[12] Muhammad, Mustapha; Bantan, Rashad AR; Liu, Lixia; Chesneau, Christophe; Tahir, Muhammad H; Jamal, Farrukh and Elgarhy, Mohammed. A new extended cosine—G distributions for lifetime studies. *Mathematics*,**9(21)**(2021),2758.

[13] Osi, A. A., Doguwa, S. I., Yahaya, A., Zakari, Y., & Usman, A., Transmuted cosine Topp-Leone G family of distributions: properties and applications. *Journal of the Nigerian Society of Physical Sciences*,(2024), 2049-2049.

[14] Odhah, Omalsad Hamood; Alshanbari, Huda M; Ahmad, Zubair and Rao, Gadde Srinivasa. A weighted cosine-G family of distributions: properties and illustration using time-to-event data. *Axioms*,**12(9)**(2023),849.

[15] Souza, Luciano; Junior, Wilson; De Brito, Cicero; Chesneau, Christophe; Ferreira, Tiago and Soares, Lucas. On the Sin-G class of distributions: theory, model and application. *Journal of Mathematical Modeling*,**7(3)**(2019),357–379.

[16] Zografos, Konstantinos and Balakrishnan, Narayanaswamy. On families of beta-and generalized gamma-generated distributions and associated inference. *Statistical methodology*,**6(4)**(2009),344–362.

© 2025 YU
Deanship of Research and Graduate Studies, Yarmouk University, Irbid, Jordan.